JOURNAL OF AIRCRAFT
Vol. 48, No. 4, July–August 2011

Hybrid Solid Oxide Fuel Cell and Micro Gas Turbine for Regional Jets

M. Santarelli*
Politecnico di Torino, 10129 Torino, Italy
and
M. Cabrera
HySyTech, SRL, 10129 Torino, Italy

DOI: 10.2514/1.C031228

Although it accounts for only 4.2% of the total global warming potential, aviation-generated CO_2 is projected to grow to approximately 5.7% by 2050, faster than any other sector. Rapidly emerging fuel-cell-based technologies could be developed for future replacement of onboard electrical systems in larger more-electric or all-electric aircraft. The Environmentally Friendly Inter City Aircraft Powered by Fuel Cells project, led by Politecnico di Torino in the Sixth Framework Programme, has carried out a feasibility study on all-electric intercity aircraft to provide a preliminary definition of new forms of aircraft systems that can be obtained by fuel cell technologies. Solid oxide fuel cell systems could be advantageous for some aeronautical applications, due to their capability of accepting hydrocarbons fuels with lower pollutant effects (e.g., natural gas), especially sustainable biofuels such as second-generation bioethanol. In this paper, the design of a hybrid solid oxide fuel cell and micro gas turbine energy system, as well as the simulation of complete missions of a regional jet, has been performed. The system will be discussed in two fuel configurations, natural gas and bioethanol, and the difference in the system structure and regulation will be discussed. Preliminary estimations on size and weight of these new systems have been carried out. The obtained results are discussed.

Nomenclature

F	=	Faraday number, $C\,mol^{-1}$
G	=	mass flow, $kg\,s^{-1}$
h	=	specific enthalpy, $kJ\,kg^{-1}$
$\bar{h}$	=	molar enthalpy, $kJ\,mol^{-1}$
I	=	generator current intensity, A
n_c	=	number of cells
S	=	single-cell active area, cm^2
U_f	=	fuel utilization factor in coded form
U_{ox}	=	air utilization factor in coded form
V_c	=	single-cell voltage, V
W_{DC}	=	stack electrical power, kW
x	=	moles of CH_4 that react, $mol\,s^{-1}$
y	=	moles of CO that react, $mol\,s^{-1}$
$\Delta\bar{h}_{react}$	=	molar enthalpy of chemical reaction, $J\,mol^{-1}$
$\eta_{act,a/c}$	=	activation overpotential at anode and cathode, V
$\eta_{conc,a/c}$	=	concentration overpotential at anode and cathode, V
η_{ohm}	=	ohmic overpotential, V
Φ_{air}	=	heat for oxidant (air) preheating, kW
Φ_{diss}	=	heat losses from the complete system, kW
Φ_{ech}	=	heat of electrochemical reaction, kW
Φ_{ref}	=	heat of steam-reforming reaction, kW
Φ_{shift}	=	heat of water shift reaction, kW

I. Introduction

ALTHOUGH aviation accounts for only 4.2% of the total global warming potential, the concern today is that aviation-generated CO_2 is projected to grow to approximately 5.7% by 2050. Aviation emissions are growing faster than any other sector and they risk undermining the progress achieved through emission cuts in other areas of the economy.

As new progress is made and fuel cell technology continues to mature, more sectors of the industry are getting interested in this topic and more private and governmental funds are being deployed for research programs that can come up with significant innovations that make fuel-cell-based systems more competitive toward traditional energy systems. In a previous paper [1], it was established how fuel cell systems could represent a good alternative for reversing the growing trend of pollutant emissions from aviation by improving efficiency or employing more environmentally friendly fuels (not only hydrogen, but also natural gas and, especially in the future, biofuels).

The ENFICA-FC (Environmentally Friendly Inter City Aircraft powered by Fuel Cells) has been a project led by Politecnico di Torino in the Aeronautics and Space priority of the EU Sixth Framework Programme Research and industrial Consortium partners of ENFICA-FC aimed at developing and providing operational zero-pollution solutions to the immediate needs of aircraft services. The project ended in June 2010 with a successful flight test of the ultralight aircraft using a powertrain with a 20 kW polymer electrolyte membrane (PEM) fuel cell stack [2].

Another objective of ENFICA-FC was to carry out a feasibility study on intercity aircraft (e.g., regional jet, 32 seats) to provide a preliminary definition of new power-supply systems based on fuel cell technologies, because they could represent an interesting alternative to the traditional thermal power systems in terms of efficiency and of environmental care.

If a simple fuel cell system is considered, [1] explains how the power consumption of an electric air compressor operating at high altitude (necessary to feed the cathode compartment of the stack with reactant air at sufficient pressure) has a significant impact over the nominal power of the stack. Integrating the stack with a micro gas turbine (μGT) bottoming cycle not only improves efficiency, but also eliminates the necessity for the electric compressor. In this sense, high-temperature fuel cells like solid oxide fuel cells (SOFCs) are the most adapted for being used in such hybrid systems.

Hybrid SOFC/μGT systems have been studied by various authors, and different models have been developed [3–5]. Some of these models have been compared and validated with actual measurements

Received 4 September 2010; revision received 20 December 2010; accepted for publication 20 December 2010.

*Dipartimento di Energetica, Corso Duca degli Abruzzi 24; massimo.santarelli@polito.it.

from operating units [6,7]. In these last two references, the model has been validated with measured data from the 220 kW SOFC/GT hybrid system developed by Siemens-Westinghouse. Nevertheless, most of the published models refer to hybrid systems for stationary applications. The hybrid SOFC/μGT technology still represents a challenge in aviation, since the system design must be adapted to the needs of aerospace applications (light weight, low air density, etc.). Interesting works regarding the use of hybrid systems in aviation have been published. In [8] the possibility of using hybrid systems in aerospace applications is introduced. In [9] parametric mass and volume models linking the thermodynamic model to the mass and volume model of a SOFC/μGT auxiliary power unit (APU) have been developed; such models provide immediate feedback during the design process. A planar anode-supported cell design stack with a gas turbine bottoming cycle APU for a 300-passenger commercial transport aircraft is analyzed in [10].

In addition to increasing efficiency, aviation is aiming to the use of alternate fuels as a strategy for reducing economic and environmental costs. In fact, since travel growth is predicted to continue at 5% per year, gains in fuel efficiency could be outpaced by the projected growth in air traffic, causing an increase of fuel consumption. Alternate fuels, object of studies by public agencies and private companies, can be divided in synthetic fuels and biofuels. Synthetic fuels are manufactured from coal, natural gas, or other hydrocarbon feedstocks. Although very similar in performance to conventional jet fuel, these fuels contain almost zero sulfur and aromatics. However, when taking into account not only final-use emissions but the entire life cycle (well-to-wheel analysis), it is found that large quantities of energy are used during the manufacturing process (well-to-tank step). According to one of the most important reports in that topic (the CONCAWE Report, [11], in which 114 different well-to-tank pathways have been analyzed in depth), it is possible to conclude that during the well-to-tank phase of their production, the synthetic fuels cause greenhouse-gas emissions, which, compared with oil derived fuels, are 1) from 95 to 120% higher in the case of gas-to-liquid (from natural gas), depending on the transport of the natural gas itself and 2) from 130 to 225% higher in the case of coal-to-liquid (from coal), depending on whether carbon capture and storage are considered or not.

With regard to biofuels, these fuels are usually plant-based, but could also be derived from other biomass sources including food and agricultural waste, lumber from timber and forestry, and animal fats. The CO_2 cycle of biofuels is considered to be environmentally balanced, theoretically annulling the impact of final-use emissions (balanced well-to-wheel CO_2 emissions). Theoretically, the ultimate advantage of biofuels is their capability to become a renewable and sustainable fuel. Some drawbacks of biofuels are the propensity to freeze at normal operating cruising temperatures, poor high-temperature thermal stability (characteristics in the engine), and poor storage stability over time.

In addition to these technical aspects (and perhaps more challenging), there is a logistical, and even political, issue of continuous discussion: the lack of enough crops for supplying the entire aviation demand for biofuels. More precisely, the issue lies in the fact that rendering biofuels sustainable would require the deployment of large areas of land and other resources like water, fertilizer and manpower. First-generation biofuels (produced primarily from food crops) are not able to counteract oil-product substitution. On the other hand, there are large expectation from second-generation biofuels produced from nonfood biomass, such as cereal straw, forest residues, and purpose-grown energy crops such as vegetative grasses and short rotation forest, but there are still important technical barriers to adopt second-generation biofuels. In this context, higher expectations of sustainability are linked to the third generation biofuels, produced by micro-algal biomass cultures, which avoids competition with other productive land uses. However, there is not yet a clear view of the potential for the technologies or any consensus about the optimum role for algae, with many algal strains and routes to energy under consideration.

Despite the questions regarding the effect on human food chain, continuous research on biofuels is being carried out by aircraft industries around the world and big achievements have been made in the last few years. In January 2009, Continental Airlines successfully completed a test flight of an unmodified Boeing 737-800 with one of its two engines running on a mixture of 50% biofuel and 50% aviation jet fuel [12].

In November 2008 Air New Zealand also reported a successful test flight, this time of a 747-400 with one of its four engines powered by fuel consisting of 50% jet fuel and 50% biofuel [13]. The test flight was a joint initiative between Air New Zealand, Boeing, Rolls Royce, and UPO, which is owned by Honeywell. A few months earlier, Virgin Atlantic Airways flew a Boeing 747-400 from London to Amsterdam with one of its four tanks filled with jet fuel containing a 20% blend of biofuel. Based on this promising trend, it is reasonable to think that we are not so far from the first only-biofuel-powered flight.

An extensive up-to-date overview of completed alternative-fuel flight tests is provided in [13].

The biofuels can be used in different options of power systems, but a high interest is assigned in the coupling of solid oxide fuel cells and biofuels, due to the high conversion efficiency and other technical reasons. In fact, this coupling would take advantage of the high conversion efficiency of the fuel cells (higher than the efficiency achieved by the utilization of biofuels in thermal engines) and, in particular, of the high operating temperature of the SOFC and the efficient recovery of its waste high-temperature irreversible heat for thermal integration and system performance enhancement. The utilization of biofuels in SOFC has still many problems to be solved (essentially linked to anode degradation with time), but it represents a very interesting option for the future, both in the stationary and in the transportation sectors [14]. Nevertheless, the authors have already made many experimental experiences on the use of biogas and vaporized biofuels in SOFC anodes; the results demonstrate that if the biofuel is vaporized and properly reformed (with high steam-to-carbon ratios to avoid C deposition in the reformer bed and in the following anode layer of the SOFC stack) in a reactor before the stack inlet, the obtained mixture can be safely and efficiently used in the SOFC stack [15]. Therefore, this option has been taken into account in the evaluation done in the ENFICA-FC project.

In this paper, a hybrid SOFC/μGT energy system model is designed and the simulation of complete missions has been performed for an intercity aircraft (regional jet, 32 seats). Mission profiles correspond to those presented in a previous work [1]. Two cases have been analyzed and compared: one in which the hybrid system is fed on natural gas (a less pollutant hydrocarbon fuel, with higher energy density than other gaseous fuels), and one regarding the use of liquid ethanol, considered an environmentally friendly fuel when obtained from biological processes (bioethanol). Preliminary estimations on size and weight of these systems have been carried out. The obtained results are discussed.

II. Case Study

Other than the demonstrator, three different types of aircraft have been object of study of the ENFICA-FC project: air taxi (five seats, 500 kg payload), small commuter (9 seats, 1823 kg payload), and regional jet (32 seats, 3410 kg payload) [1]. For these three types, work has been focused on the feasibility of supplying the onboard loads of passenger planes with SOFC-based systems. As for the air taxi and small commuter, the use of a hybrid SOFC/μGT system seems to be impractical because of the small size of the resultant turbine; this solution could be more appropriate for the regional jet, for which electrical load reaches peaks of more than 60 kW along a mission.

The mission profile analyzed in this work, presented in Fig. 1, is the same profile analyzed in [1] and deeply explained in [16]. The peak electrical load, determining the nominal power of the system, is 62.4 kW. This peak load corresponds to the phases of takeoff, climb, and descent. The electrical load during the cruise phase is 44.6 kW and could be considered as the steady state of the system.

Apart from the electric loads, the heating system of the passenger cabin requires about 20 kW in form of thermal power. Therefore,

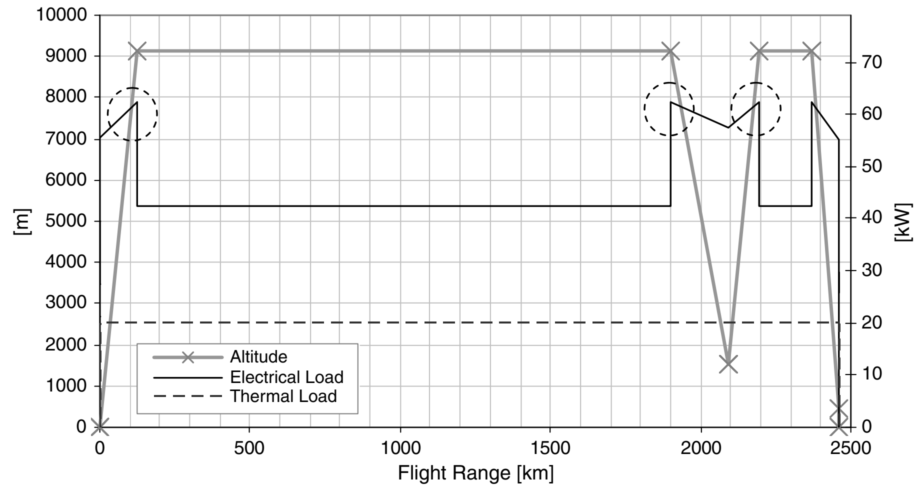

Fig. 1 Regional jet mission profile.

other than the electric load, the hybrid system has to supply the 20 kW of thermal power in most of the mission phases.

The possibility of operating under a combined heat-and-power configuration is one of the main advantages of high-temperature fuel cells like SOFC over other kinds of fuel cell like PEM systems, in which the waste heat is not very useful, because it is available only at low temperatures (nearly 60°C). Nevertheless, the main advantage of the high-temperature operation is to make it easier to couple the SOFC system with the gas turbine, which exploits the energy content of the stack exhausts.

III. Hybrid SOFC-μGT Plant: Gaseous and Liquid Fuels

A planar SOFC stack is the base of the energy system analyzed in this work. This cell geometry offers better electrochemical performance when compared with other geometries (tubular and delta) that suffer high ohmic overpotential due to long electron paths [16]. In addition, planar cells are more compact and light, so this type of cell is considered to be the one that better suits the requirements of aeronautical applications. The single cell is anode-supported, and composed of standard materials: 500–520 μm NiO/8YSZ (Yttria-stabilized zirconia) anode support, a 4–6 μm 8YSZ electrolyte, a 14–16 μm lanthanum strontium manganite oxide (LSM)/8YSZ cathode active layer, and a 18–20 μm pure-LSM current collector layer.

With regard to the SOFC stack, it is integrated with a catalytic reformer for the internal reforming of the fuel; part of the anode exhaust gas is recirculated in the fuel stream using an ejector, in order to supply the electrochemically produced water for use in the fuel reforming. The system is integrated with other auxiliaries (first, a desulphurization bed of the fresh fuel, usually composed of zeolites, ejectors, heat exchangers, blowers, valves, etc.), defined as the balance of plant (BOP). A schematic flow of the stack arrangement, with its BOP, is shown in Fig. 2.

The complete plant is a hybrid system that consists of a SOFC plant integrated with a micro gas turbine bottoming cycle; its schematic process flow diagram is reported below with the related thermodynamic states. The process gas from the SOFC (both anode and cathode exhaust) passes through a postcombustion chamber. Subsequently, it is sent into the expansion turbine, which drives the integrated air compressor and provides its net electrical power to the onboard loads, reducing the load (and therefore the size) of the SOFC stack. Exhaust gas from the turbine (flow 08) is then used for preheating the compressed air, for supplying heat to the fuel processing system (fuel conditioning), and for supplying thermal energy through a heat-recovery system.

The operating pressure of the stack is set to about 5.6 barg to allow the exhaust expansion throughout the turbine, obtaining a good tradeoff between compression power and system performance [5]. In fact, an operating pressure higher than atmospheric translates to cell performance improvement (due to Nernst effect). Moreover, a better cell performance means less heat generated by irreversibility reducing the amount of excess air for controlling the stack temperature and consequently the power needed for air compression.

It has been hypothesized the use of air from the passengers' cabin (flow 13) for feeding the stack, significantly reducing the compression ratio (and the power) for the air compression and with it the size and weight of the μGT and consequently of the stack. Passengers' breathing has been proved not to affect the performance of the stack [16].

The reason for including a postcombustion chamber between the stack and the turbine is to achieve a better performance of the μGT by increasing its inlet temperature (flow 05). In addition, this measure makes it possible to control the temperature at the turbine inlet; in fact, controlling this temperature with only the operating temperature of the stack could be a rather complex issue. This solution, on the other hand, adds another fuel-consuming component to the system. The weight of the new components, as well as their fuel consumption should be accounted for if the hybrid system is to be compared with the only-SOFC solution.

The exhaust temperature, downstream of the micro gas turbine (flow 08), has the constraint of ensuring the closure of the thermal balance (air preheating, fuel processing, heat recovery); it is

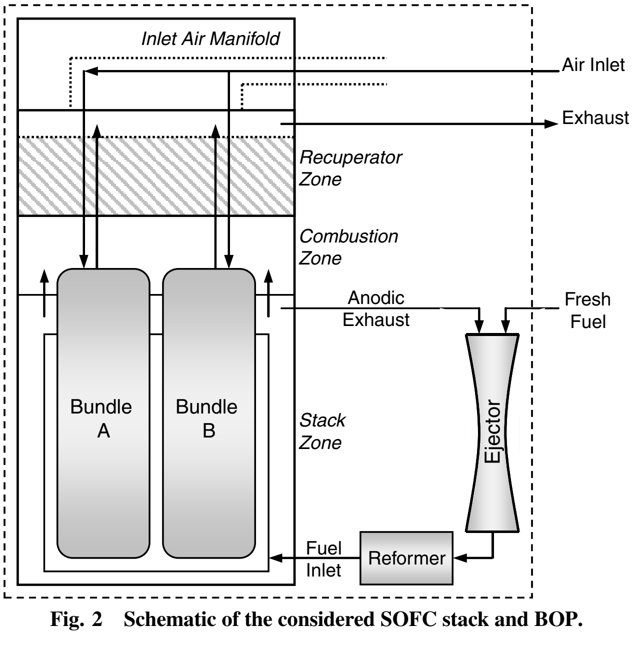

Fig. 2 Schematic of the considered SOFC stack and BOP.

Table 1 Comparison between the considered fuels and hydrogen

	Low heating value, MJ/kg	Density, kg/m^3	Energy content, MJ/m^3
Hydrogen	120	Gas: 0.084 (23.7) @350 bar	Gas: 11 (3.5×10^3) at 350 bar
Natural gas	45	Gas: 0.717 (237.2) @350 bar	Gas: 32 (11×10^3) at 350 bar
Bioethanol	26.7	Liquid: 789	Liquid: 21×10^3

controlled with a fraction of combusted exhaust that bypasses the turbine (flow 07).

The stack temperature, on the other hand, is controlled by varying its air utilization (excess air).

A. Considered Fuels

One of the main features of SOFCs is that they run on hydrocarbons (although they could perfectly run on pure hydrogen, provided that the thermal balance of the system is assured). The advantage lies on the fact that these fuels are denser and more stable, so the same amount of energy can be stored in smaller volumes avoiding the complexity and the hazards related to the storage of hydrogen as compressed gas or in its liquefied form, as well as the energy spent for compression or liquefaction.

In this work, two types of fuel have been considered: natural gas and bioethanol. The main characteristics of these fuels are summarized in Table 1. Natural gas is the most commonly used in SOFC. When operating on natural gas, no particular fuel processing is needed (before the stack internal reforming) and the fuel is sent directly into the in-stack reformer before the electrochemical reaction in the stack.

Among possible liquid fuels, ethanol (C_2H_5OH) has a high hydrogen-to-carbon ratio. Theoretically, six moles of hydrogen can be obtained from the reforming of 1 mol of ethanol.

Steam reforming:

$$C_2H_5OH + 2H_2O \rightarrow 4H_2 + 2CO \tag{1}$$

Water–gas shift:

$$CO + H_2O \rightarrow H_2 + CO_2 \tag{2}$$

A liquid fuel, however, cannot be sent directly into the SOFC stack. Ethanol should be evaporated and superheated upstream from the stack. To this end, heat from the exhaust is used to supply the fuel-conditioning reactor observed in the schematic diagram below in the text.

Finally, with both the fuels a process of desulphurization has to be performed before sending the stream to the in-stack reformer. This is composed of an adsorption bed made by zeolites, removing the H_2S traces in the fuels to values below 1 ppm. The adsorption bed is included in the balance of plant of the SOFC system.

B. Model

With the load profile of the onboard loads of a regional jet for a typical mission [1,16], the complete mission can be simulated through a computer-based model that takes into account the electrochemical behavior of the stack, the chemical model and the thermodynamic balances applied to each single component of the system.

The composition of the gas stream supplied to the anode of the stack is evaluated considering the processing of the primary fuel (flow 03) in the internal reforming reactor (Fig. 2); in stationary conditions, the composition is evaluated by imposing the chemical equilibrium at the reactor's temperature, which is found by imposing the minimization of the total Gibbs free energy of the reactive mixture. Furthermore, it has been imposed the conservation of atomic species, with the aid of Lagrange's multipliers [14,17–21], obtaining the system of nonlinear Eqs. (3):

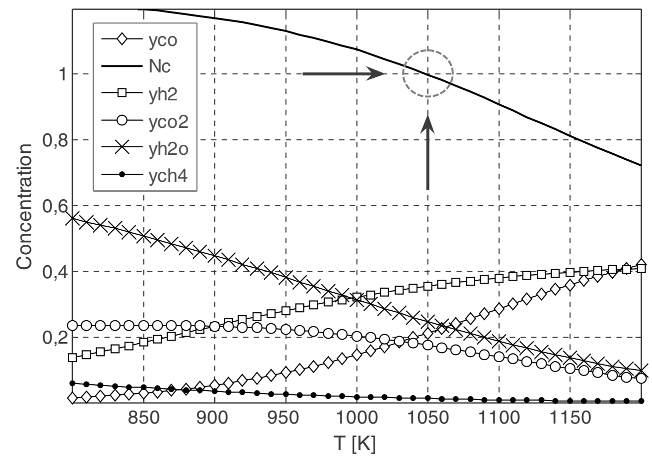

Fig. 3 Concentration of chemical species in the gas stream arriving at anode surface, as a function of temperature (in the case of primary fuel composed of ethanol/water 75/25% mol).

$$\Delta G^0_{f_i}(T) + RT \cdot \ell n \frac{y_i \cdot P}{P_0} + \sum_k \lambda_k \cdot a_{ik} = 0 \tag{3}$$

where $\Delta G^0_{f_i}(T)$ is the standard Gibbs energy of formation of species i as a function of temperature, y_i is the gas-phase mole fraction, P_0 is the standard-state pressure of 101.3 kPa, P is the stream pressure, a_{ik} is the number of atoms of species i in reaction k, and λ_k is the Lagrange multiplier applied to reaction k.

With regard to ethanol, the fresh fuel is not pure ethanol, but a mixture of ethanol and water. This approach comes out from the necessity to avoid carbon deposition on the reforming reactor, especially on the anode surface, which is a harmful phenomenon that causes irreversible damages. Thus, considering the concentration of chemical species as a function of the temperature and composition of the fresh fuel, it can be identified the range of conditions (composition of primary fuel and temperature) in which carbon deposition can be avoided. From the analysis on ethanol steam reforming, it has been established, at the imposed stack temperature of operation (800°C), the composition of liquid fresh fuel: 75% ethanol, 25% water on molar basis; it has to be noted that this is a conservative composition to avoid any problem of C deposition. In Fig. 3, in the case of ethanol/water mixture of 75/25 (molar basis), the composition of the fuel gas after the reforming (thus, at the anode surface) as a function of temperature is reported, showing the absence of C deposition at the stack operating temperature of 800°C. Fuel composition at the anode surface, when operating on the aforementioned conditions, is presented in Table 2.

Table 2 also shows the fuel composition at the anode surface when feeding the stack on natural gas, in this case, even processed through a steam-reforming reaction to avoid C deposition.

The electrochemical behavior of the stack (polarization) has been modeled on the basis of experimental polarization curves of anode-supported cells tested on the test bench of the high-temperature fuel cell laboratory in the Energetics Department of Politecnico di Torino. To this end, the polarization is performed imposing the gas

Table 2 Concentration of chemical species at anode surface in the case of the two primary fuels

	Composition, %	
	Natural gas	Ethanol
CH_4	1.9	1.1
H_2	43.2	36.5
CO	17.5	20.4
CO_2	11.8	16.1
H_2O	25.6	25.9

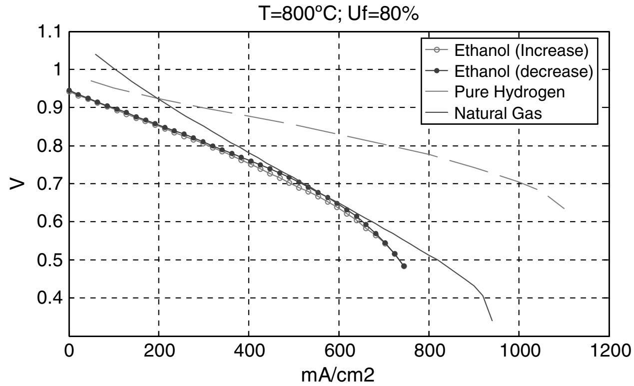

Fig. 4 Polarization of planar cells fed with reformed natural gas and reformed ethanol/water mixture.

composition (downstream of the steam reforming) and the cell temperature (see Fig. 4).

As evident in Fig. 4, the natural gas fuel performs a better polarization than with ethanol fuel (hydrogen fuel is used as a reference). In fact, considering the anode mixture composition (Table 2), the mixture obtained from the processed natural gas fuel has a higher H_2 and a lower CO fraction; this causes a better reaction kinetic (lower anode activation polarization). The mixture obtained from the processed natural gas fuel also has a lower CO_2 fraction; this means that the diffusion mechanisms of the electrochemically reactant species (H_2, CO), both in the bulk flow and in the porous electrode, are enhanced. In fact, the molecules diffuse better in mixtures with low molecular mass chemical species; a high fraction of CO_2 in the mixture (molecular mass 44 g/mol) causes a reduction of the diffusion and therefore an increase of the anode concentration polarization. This is evident in Fig. 4, where the anode mixture obtained from the processed ethanol fuel reaches lower current density levels because of the higher fraction of CO_2 in the mixture.

A very generalized expression of the polarization curve for a solid oxide fuel cell is

$$V_c = E_{\text{rev}} - \eta_{\text{act},a/c} - \eta_{\text{ohm}} - \eta_{\text{conc},a/c} \tag{4}$$

where V_c is the single-cell voltage, E_{rev} is the reversible (open-circuit) voltage, $\eta_{\text{act},a/c}$ is the activation overpotential, η_{ohm} is the ohmic overpotential, and $\eta_{\text{conc},a/c}$ the concentration overpotential. The considered equations for the polarization of anode-supported planar SOFC are reported in [18–21] and summarized next; some papers have been taken into account in setting some specific parameters such as porosity and tortuosity [22,23]. The characteristic parameters of the overpotential expressions have been found from nonlinear regressions of the experimental curves performed in the laboratory tests performed at Politecnico [1,16].

Activation overpotential $\eta_{\text{act},a/c}$ for cathodes is

$$\eta_{\text{act},c} = \frac{RT}{\alpha_c F}\ \sinh^{-1}\left(\frac{i_c}{2i_{0,c}}\right)$$

Activation overpotential $\eta_{\text{act},a/c}$ for anodes is

$$\eta_{\text{act},a} = \frac{RT}{\alpha_a F}\ \sinh^{-1}\left(\frac{i_c}{2i_{0,c}}\right)$$

Ohmic overpotential ($\eta_{\text{ohm}} = i_c \Sigma_j r_j$, where $r_j = \rho_j t_j$ and t_j is the path of the charged particle) is $\rho_a = 0.008114 \exp(600/T)$ for anodes, $\rho_{\text{el}} = 0.00294 \exp(10,350/T)$ for electrolytes, $\rho_{c,\text{ccl}} = 0.0017 \exp(1280/T)$ and $\rho_{c,\text{fl}} = 0.0079 \exp(10,350/T)$ for cathodes (current collector layer and functional layer), and $\rho_{\text{int}} = 0.1256 \exp(4690/T)$ for the interconnection.

Concentration overpotential for anodes and cathodes is

$$\eta_{\text{conc},a/c} = \frac{RT}{nF}\,\ell n\left(1 - \frac{i}{i_{l,a/c}}\right)$$

Concentration overpotential for anodes is

$$i_{l,a} = \frac{2 \cdot F \cdot p^b_{H_2} \cdot D_{a(\text{eff})}}{R \cdot T \cdot t_a}$$

Concentration overpotential for cathodes is

$$i_{l,c} = \left(4 \cdot F \cdot p^b_{O_2} \cdot D_{c(\text{eff})}\right) \Big/ \left[\left(\frac{p - p^b_{O_2}}{p}\right) R \cdot T \cdot t_c\right]$$

$$D_{a/c(\text{eff})} = \frac{\varepsilon_{a/c,\text{fl/ccl}}}{\tau_{a/c}} \cdot D^{293\text{ K}}_{i-j} \cdot \left(\frac{T}{293}\right)^{1.5}$$

where the constants $\alpha = 1.4$, anode porosity $\varepsilon_a = 0.25$, cathode current collector-layer porosity $\varepsilon_{c,\text{ccl}} = 0.30$, cathode functional-layer porosity $\varepsilon_{c,\text{fl}} = 0.10$, anode tortuosity $\tau_a = 2.5$, and cathode tortuosity $\tau_c = 2.5$.

Six main blocks compose the hybrid system: SOFC stack and BOP, postcombustor, micro gas turbine, fuel conditioning, fuel storage, and heat-recovery system.

The fresh fuel is flow 01-02; in the case of natural gas, it can be sent directly to the BOP of the stack (exactly in the desulphurization bed and consequently in the steam-reforming reactor); in the case of hydrated ethanol fuel (75% ethanol and 25% water) in liquid phase, it cannot be sent directly into the stack, and therefore heat from the exhaust is used for evaporating and superheating the fuel in the fuel-conditioning block. The fuel (flow 03) is then desulphurized, reformed in the in-stack reformer, and subsequently converted electrochemically in the SOFC stack producing the main electric power, and the air-rich exhausts (from anode and cathode; flow 04) are sent to the postcombustor block. Another mass flow of fresh fuel (flow 12; natural gas, or pure ethanol, since there is no problem of avoiding C deposition such as in the stack) is fed to the postcombustor upstream of the gas turbine, in order to keep the turbine inlet temperature constant and to increase the temperature of the streams 05 and 07 to have enough heat for the thermal balance of the complete plant; in fact, the exhaust temperature downstream of the GT (flow 08) which ensures the closure of the thermal balance (air preheating, fuel conditioning, heat recovery) is controlled with a fraction of the combusted exhaust that bypasses the GT (flow 07).

The postcombustor main stream (flow 05) is expanded in the gas turbine, which produces more-electric power and which moves the air compressor supplying cathode air at the correct pressure to the SOFC stack (flow 14 preheated in flow 15 to avoid thermo-mechanical problems in the SOFC cells). The cathode air is also used for thermal regulation of the stack; in fact, stack temperature is controlled by varying its air utilization factor (excess air). As described above, it has been hypothesized the use of cabin air for feeding the stack.

The GT exhausts, after being used for air preheating and fuel conditioning, are sent to the heat-recovery block (flow 10), in order to recover the residual heat for internal loads of the aircraft.

The design of every component has been performed. The model considers a zero-dimensional approach. Steady-state conditions have been assumed.

The balance of plant has been modeled as explained in [1]. Devices that define the SOFC plant (micro gas turbine, heat exchangers, postcombustor, etc.) are defined by energy balance equations applied to each component and by thermodynamic equilibrium in the case of chemical reactions.

IV. Results

In Fig. 5 the schematic diagram of the plant is shown with the main thermodynamic values of the transformations.

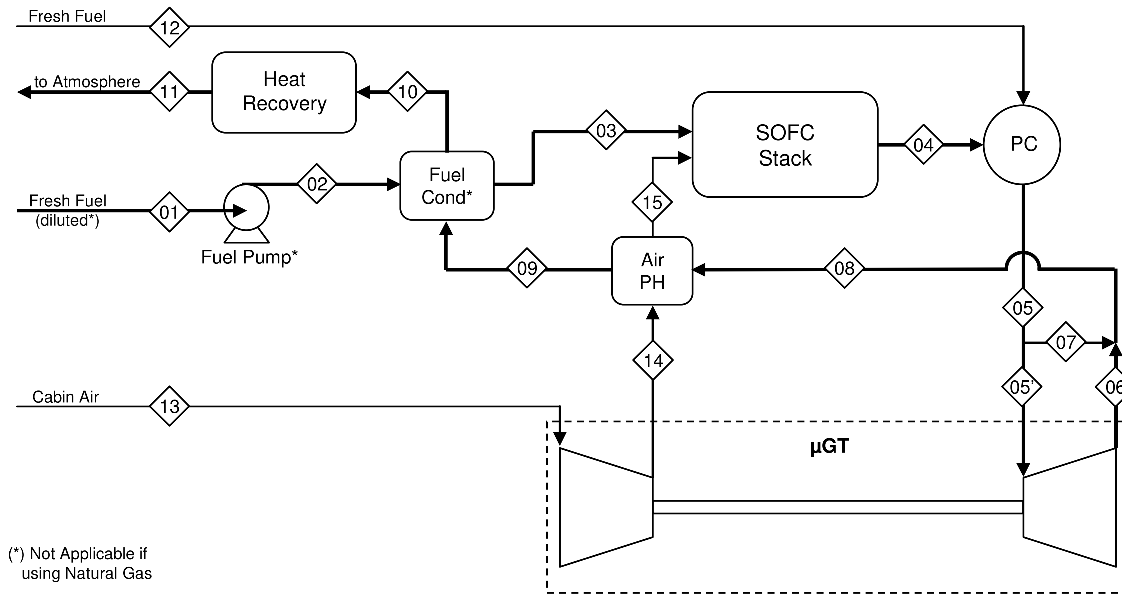

Ethanol

Stream	01	02	03	04	05	06	07	08	09	10	11	12	13	14	15
Description	Fuel (diluted)	Fuel	Fuel	Cell Exhaust	Combusted	Turbine Exhaust	Combusted	Exhaust	Exhaust	Exhaust	Exhaust	Fuel	Cabin Air	Compressed Air	Feed Air
Temperature [ºC]	15	15	142	800	1300	599	1300	858	433	401	110	15	22	303	600
Pressure [bar]	0.8	6.6	6.6	6.6	6.6	0.3	0.3	0.3	0.3	0.3	0.3	6.6	0.8	6.6	6.6
Flowrate [kg/h]	8.3	8.3	8.3	290.2	292.6	184.4	108.3	292.6	292.6	292.6	292.6	2.4	281.9	281.9	281.9

Natural Gas

Stream	01	02	03	04	05	06	07	08	09	10	11	12	13	14	15
Description	Fuel	NA	NA	Cell Exhaust	Combusted	Turbine Exhaust	Combusted	Exhaust	Exhaust	NA	Exhaust	Fuel	Cabin Air	Compressed Air	Feed Air
Temperature [ºC]	15	NA	NA	800	1300	599	1300	789	357	NA	110	15	22	303	600
Pressure [bar]	6.6	NA	NA	6.6	6.6	0.3	0.3	0.3	0.3	NA	0.3	6.6	0.8	6.6	6.6
Flowrate [kg/h]	3.3	NA	NA	345.6	348.1	254.1	94.0	348.1	348.1	NA	348.1	2.5	342.3	342.3	342.3

Fig. 5 Process flow diagram of the system, in the case of both natural gas and bioethanol feeding, with main thermodynamic values.

The comparison between natural gas and ethanol has been made at the same operating conditions: stack pressure of 6.6 bar, turbine inlet temperature of 1300°C, and outlet exhaust temperature 110°C. If we compare the two typologies of primary fuels, we could note the following.

The natural gas is sent from the vessel to the BOP without any operation. Conversely, the hydrated ethanol has to be first pumped, vaporized, and superheated in the fuel-conditioning block; this operation requires heat from the exhaust gases (flow 10 pass from 433 to 401°C), which has to be considered in the energy balance.

At the same time, the natural gas fuel requires a higher air mass flow (flows 13-14-15); that is, the system operates with a higher excess air. The point is the temperature control of the stack; it is obtained by considering the presence of heat sinks (the endothermic steam-reforming reaction of the primary fuel), especially through the use of excess air. In the case of natural gas (of course, compared with ethanol), the steam-reforming reaction heat sink is lower, because of the lower mass flow of primary fuel (flow 01) and the lower endothermicity of the reaction itself. Therefore, the system requires more air. This means a higher consumption of the air compressor and also a higher mass flow of the stack exhausts (flow 04), which means a higher mass flow expanded in the turbine (flow 05) and thus more power.

The mass flow of fresh fuel in the postcombustor (flow 12) is therefore slightly lower in the case of ethanol, because the mass flow 04 to be heated to 1300°C is lower.

The exhaust temperature downstream of the GT (flow 08) is higher in the case of ethanol; this is in order to ensure the closure of the thermal balance (thermal requests of air preheating, fuel conditioning, and heat recovery), considering that its mass flow is lower. To maintain a high temperature of flow 08, the fraction of the combusted exhaust that bypasses the GT (flow 07) has to be higher in the case of ethanol fuel.

The main heat recovery is the air preheating; after this use, the exhausts are available at 433°C (ethanol fuel) or 357°C (natural gas fuel), but in both cases the temperature is enough to supply heat for internal loads of the aircraft through the heat-recovery block.

The main point to consider is that the mass flow of the primary fuel is lower in the case of natural gas. This is due mainly to the better cell electrochemical performance when supplied with reformed natural gas, already described in Fig. 5. Also, the natural gas does not need to be pumped or vaporized, thus reducing the energy requests of the system.

Therefore, the natural gas has to be preferred in terms of fuel consumption, while in general the system operates in a quite similar way with the two fuels.

Concerning the fuel consumption along the mission, Fig. 6 shows the analysis of the primary fuel (natural gas and ethanol) consumption in a complete mission, separated in SOFC/GT and postcombustor.

In the case of natural gas, the complete mission (Fig. 1) has an overall consumption of 32 kg/mission of primary fuel. The consumption can be separated in the components SOFC/GT and postcombustor. The SOFC/GT component has a consumption of 17 kg/mission of primary fuel, while the postcombustor has a consumption of around 15 kg/mission of primary fuel.

In the case of ethanol, the complete mission has an overall consumption of 53 kg/mission of primary fuel (ethanol). The SOFC/GT component has a consumption of 38 kg/mission of primary fuel, while the postcombustor has a consumption of around

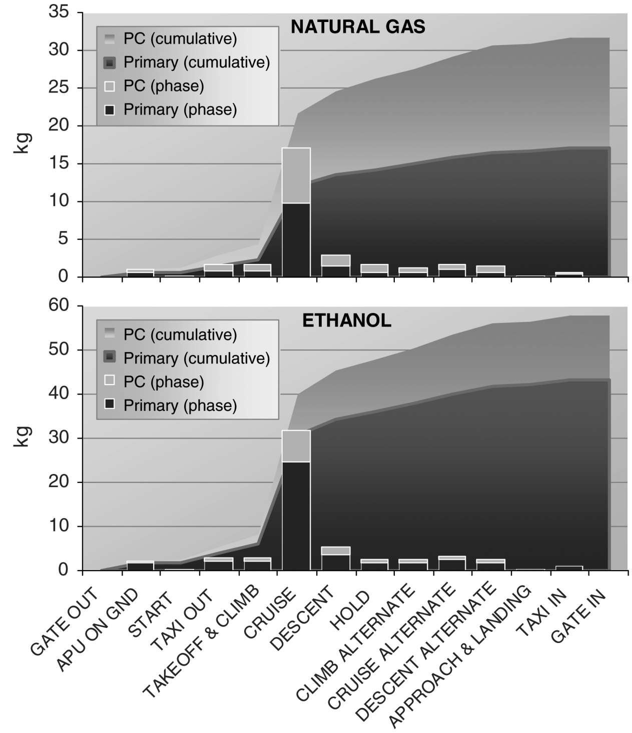

Fig. 6 Fuel consumption in a complete mission, separated in SOFC/GT and postcombustor.

15 kg/mission of primary fuel. Note that in order to protect the cell from carbon deposition, the fresh ethanol to be sent into the stack is blended with water: 5 kg of H_2O added to the 38 kg of ethanol going in the SOFC anode (for a final amount of 43 kg of mixture). Therefore, the impact of water on the total primary fuel (58 kg) is 8.6%. Actually, this water has been added to the ethanol for the sake of excess safety, because water is already present in the anode recirculation, which reacts with the fresh fuel in sufficient amount to reform the ethanol. The 5 kg of added water could be in future avoided, especially if materials avoiding C deposition are employed in the anode electrode. Of course, the water is not added to the ethanol burned in the postcombustion chamber.

As already noted, the postcombustor requires more fuel in the case of natural gas. In fact, the difference between fuel for the stack and for the postcombustor is significant in the case of natural gas (the postcombustor fuel is the 47% of the total), while in the case of ethanol the fuel for the postcombustor is limited to around 39% of the total.

When it comes to aerospace, the weight is a fundamental issue. Concerning the system, the mass of each component has been estimated separately and added for obtaining the overall weight, which can be then compared with traditional internal power-supply systems for this kind of aircraft.

With regard to the stack, it has been first calculated the mass of the single cell, taking into account the cell geometry and the thickness and composition of each layer (anode, cathode, electrolyte) found from direct measurements (SEM analysis), and the mass of the interconnect [22–24]. In particular, as expected, in planar SOFC most of the weight of the stack corresponds to the Crofer-22 interconnection plates (0.5 mm thick) between the cells [25]. The number of cells depends on the nominal power of the SOFC stack, obtained on the basis of the maximum electrical load along the regional jet's typical mission load profile [1]. In a similar way, the mass of the stack's balance of plant has been estimated according to geometry and composition of each component (ejector, internal insulation, internal vessel, etc.).

The heat-recovery system has been estimated on the basis of existing commercial units. The same approach has been employed for the gas turbine, the postcombustor, and the fuel processing unit. The size (duties, nominal power) of these components has been obtained from the simulation of the typical mission.

The fuel consumption has been obtained from the performed mission simulation. For the fuel storage onboard, the use of a regular thin-walled vessel at atmospheric pressure has been hypothesized in the case of ethanol, and type 3 (aluminum lining) gas cylinders have been hypothesized in the case of natural gas, for which the use is hypothesized at 350 barg. In this sense, the mass of the tank itself is higher in the case for the natural gas, even though the mass of the fuel alone is considerably lower.

The allocation of the overall weight of the hybrid system in the considered blocks is presented in Fig. 7.

The mass of the hybrid system can be compared with that of the traditional power-supply system of the regional jet: a 180 kg turboshaft APU. Other than the weight of the system, the fuel consumed by the traditional APU in a mission with the same range as the one treated in this work (about 83 kg of jet fuel) [26] has been taken into account. The total weight of the traditional APU, used for comparison, is therefore 264 kg (for the considered mission).

The weight obtained by the complete SOFC/μGT-based system fed by natural gas is still higher than the weight of the traditional APU (315 kg). Nevertheless, the hybrid system consumes only 32 kg of natural gas per mission, compared with the 83 kg of jet fuel of the traditional APU.

The main percentage of weight is linked to the stack plus BOP (43%), while the percentage of the fuel plus tank is 34%. The contribution of the μGT is not negligible (13%), because of the high air mass flow to be used by the stack (as already described). The innovation has to be devoted to the reduction of weight, especially of the stack and its BOP, through materials and engineering solutions (e.g., a different stack-cooling process could reduce the air mass flow and also save weight in terms of μGT).

The weight obtained by the complete SOFC/μGT-based system fed by hydrated ethanol is still higher than the weight of the traditional APU (330 kg). Nevertheless, the hybrid system consumes 53 kg of ethanol per mission, compared with the 83 kg of jet fuel of the traditional APU. The main percentage of weight is linked to the stack plus BOP (56%), while the percentage of the fuel plus tank is

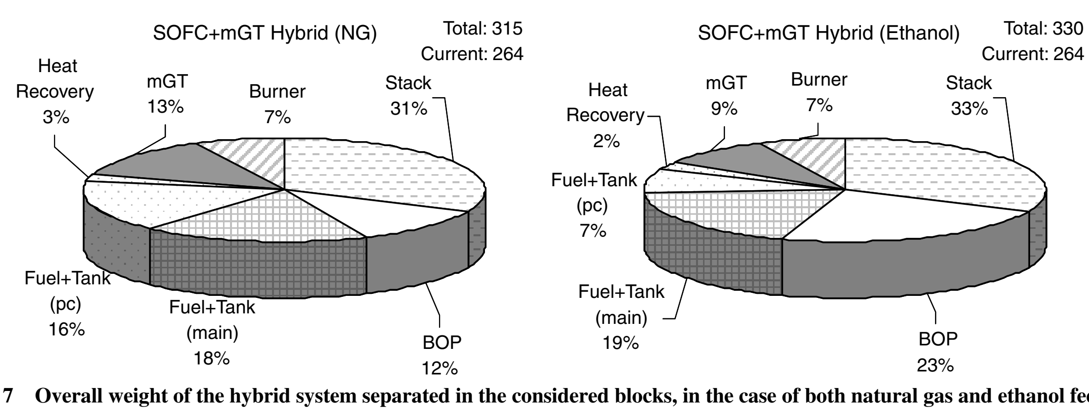

Fig. 7 Overall weight of the hybrid system separated in the considered blocks, in the case of both natural gas and ethanol feeding.

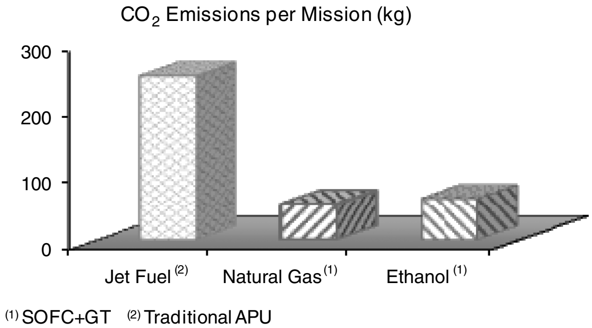

Fig. 8 Comparison of CO_2 emissions using three different fuels.

only 26%, and the μGT is very low (reduced air mass flow for stack cooling). Therefore, even in that case, the innovation has to be devoted to the reduction of weight, especially of the stack and its BOP, through materials and engineering solutions.

Typically, adding components to a system is detrimental in terms of weight. This is true in the case of liquid ethanol, where the need for prereforming increases the overall mass. On the other hand, if the hybrid system is seen as the inclusion of a μGT in the SOFC-based system, the μGT not only does not add weight, but it reduces the mass of the entire system. Weight reduction is reached by means of the high power density of the μGT, and thanks to an efficiency improvement obtained of the hybridized system; the bottoming cycle makes it possible to exploit the energy still contained in the gas stream leaving the stack.

In addition to fuel consumption, an aspect of main interest when it comes to environmentally friendly aircraft is CO_2 emissions. The use of cleaner fuels with lower carbon content, together with more efficient systems, could significantly reduce CO_2 emissions. In fact, CO_2 emissions of a traditional APU operating on jet fuel (about 250 kg for the analyzed mission profile) are almost four times those of a SOFC/μGT system fed on ethanol (about 64 kg) and close to five times those of the system SOFC/μGT APU operating on natural gas (about 55 kg). A comparison between these three cases can be seen in Fig. 8.

V. Conclusions

The paper describes the design and simulation of a hybrid SOFC/μGT energy system, fed by two alternative fuels (natural gas and bioethanol), to be used as APU in a regional jet. The analysis has been developed in the framework of the ENFICA-FC (Environmentally Friendly Inter City Aircraft powered by Fuel Cells) project led by Politecnico di Torino in the Aeronautics and Space priority of the Sixth Framework Programme.

Aviation is looking for higher efficiency and lower environmental impact.

From the efficiency point of view, the hybrid SOFC/gas turbine cycle is a potentially attractive option for aerospace applications.

From the environment point of view, aviation is aiming to the use of alternate fuels as a strategy for reducing economic and environmental costs. In this context, fuels such as natural gas or biofuels could represent an interesting option, and they can be used with high efficiency in hybrid SOFC/gas turbine cycle, as discussed in the paper.

1) The SOFC/μGT-based system fed by natural gas would have a weight (315 kg) still higher than the traditional APU fed by jet fuel (264 kg), but the SOFC system has a significantly higher efficiency (around 32 kg of natural gas per mission, compared with the 83 kg of jet fuel of the traditional APU); the fuel used also has a lower environmental impact if compared with jet fuel.

2) The SOFC/μGT-based system fed by hydrated ethanol would have a weight (330 kg) higher than the traditional APU fed by jet fuel (264 kg), but the SOFC system has a higher efficiency (around 53 kg of ethanol per mission, compared with the 83 kg of jet fuel of the traditional APU); in particular, the fuel used is a renewable and sustainable one, if compared with jet fuel.

Thus, in the case of the regional jet, the hybrid SOFC/μGT solution seems to be a good choice, especially in terms of efficiency, but it could become interesting, even in terms of mass of the overall system.

Many aspects should still be analyzed, and improvements of the fuel cells and fuel storage systems are yet to be made before this technology could be competitive with traditional and long-proven technologies (since security and reliability of every component is a major issue when it comes to aeronautics). Some characteristic conditions of aeronautical applications are new in the field of fuel cells, for long employed in stationary power production and automotive applications.

Acknowledgments

The authors acknowledge the European Commission (EC) support through the Environmentally Friendly Inter City Aircraft Powered by Fuel Cells (ENFICA-FC) project, EC 6th Framework Programme, contract no. AST5-CT-2006-030779. The authors would also like to thank all ENFICA-FC partners.

References

[1] Santarelli, M., Cabrera, M., and Calì, M., “Fuel Cells in Aeronautics: Analysis of SOFC Systems for More-Electric Aircraft,” *Journal of Aircraft*, Vol. 46 No. 1, pp. 269–284. doi:10.2514/1.38408, 2009.

[2] Romeo, G., Cestino, E., Borello, F., and Correa, G., “An Engineering Method for Air-Cooling Design of 2-Seat Propeller Driven Aircraft Powered by Fuel Cells,” *Journal of Aerospace Engineering* (to be published).

[3] Costamagna, P., Magistri, L., and Massardo, A. F., “Design and Part-Load Performance of a Hybrid System Based on a Solid Oxide Fuel Cell Reactor and a Micro Gas Turbine,” *Journal of Power Sources*, Vol. 96, pp. 352–368. doi:10.1016/S0378-7753(00)00668-6, 2001.

[4] Chan, S. H., Ho, H. K., and Tian, Y., “Modeling of Simple Hybrid Solid Oxide Fuel Cell and Gas Turbine Power Plant,” *Journal of Power Sources*, Vol. 109, pp. 111–120. doi:10.1016/S0378-7753(02)00051-4, 2002.

[5] Xiang, J., Calì, M., and Santarelli, M., “Calculation for Physical and Chemical Exergy of Flows in Systems Elaborating Mixed-Phase Flows and a Case Study in an IRSOFC Plant,” *International Journal of Energy Research*, Vol. 28, pp. 101–115. doi:10.1002/er.953, 2004.

[6] Yi, Y., Smith, T., Brouwer, J., Rao, A., and Samuelsen, S., “Simulation of a 220 kW Hybrid SOFC Gas Turbine System and Data Comparison,” *Proceedings of the 203rd Meeting of The Electrochemical Society*, Paris, 2003.

[7] Roberts, R. A. and Brower, J., “Dynamic Simulation of a Pressurized 220 kW Solid Oxide Fuel-Cell-Gas-Turbine Hybrid System: Modelled Performance Compared with Measured Results,” *Journal of Fuel Cell Science and Technology*, Vol. 3 No. 1, pp. 18–25. doi:10.1115/1.2133802, 2006.

[8] Freeh, J. E., Pratt, J. W., and Brower, J., “Development of a Solid-Oxide Fuel Cell/Gas Turbine Hybrid System Model for Aerospace Applications,” NASA TM—2004-213054.

[9] Tornabene, R., et al., “Development of Parametric Mass and Volume Models for an Aerospace SOFC/Gas Turbine Hybrid System,” NASA TM-2005-213819, 2005.

[10] Steffen, C. J., et al., “Solid Oxide Fuel Cell/Gas Turbine Hybrid Cycle Technology for Auxiliary Aerospace Power,” NASA TM-2005-213586, 2005.

[11] “Well-to-Wheels Analysis of Future Automotive Fuels and Powertrains in the European Context: Well-to-Tank Report,” European Commission Joint Research Center, Inst. for Environment and Sustainability, WTT Rept. 030506.doc, Ispra, Italy, 2007.

[12] Austin, A., “Boeing Planes Successfully Fly with Biofuels,” *Biodiesel Magazine* [online magazine], Jan. 2009, http://www.biodieselmagazine.com/articles/3141/boeing-planes-successfully-fly-with-biofuels.

[13] Blakey, S., Rye, L., and Wilson, C. W., “Aviation Gas Turbine Alternative Fuels: A Review,” *Proceedings of the Combustion Institute*, Vol. 33, No. 2, 2010, pp. 2863–2885. doi:10.1016/j.proci.2010.09.011

[14] Leone, P., Lanzini, A., Santarelli, M., Calì, M., Sagnelli, F., Boulanger, A., Scaletta, A., and Zitella, P., “Methane-Free Biogas for Direct Feeding of Solid Oxide Fuel Cells,” *Journal of Power Sources*,

Vol. 195, pp. 239–248.
doi:10.1016/j.jpowsour.2009.06.108, 2010.

[15] Lanzini, A., Santarelli, M., and Orsello, G., "Residential Solid Oxide Fuel Cell Generator Fuelled by Ethanol: Cell, Stack, and System Modeling with a Preliminary Experiment," *Fuel Cells—From Fundamentals to Systems*, Vol. 10 No. 4, pp. 654–675. doi:10.1002/fuce.201000004, 2010.

[16] Santarelli, M., Cabrera, M., and Calì, M., "Solid Oxide Fuel Based Auxiliary Power Unit for Regional Jets: Design and Mission Simulation with Different Cell Geometries," *Journal of Fuel Cell Science and Technology*, Vol. 7, No. 2, 2010, Paper 021006. doi:10.1115/1.3176282

[17] Gyftopoulos, E. and Beretta, G. P., *Thermodynamics: Foundations and Applications*, Macmillan, New York, 1991.

[18] De Benedictis, F., Gariglio, M., Delloro, F., Santarelli, M., Orsello, G., and Calì, M., "Methane Dilution Effect on a 5 kW Tubular SOFC System," *ECS Transactions*, Vol. 17 No. 1, pp. 175. doi:10.1149/1.3142747, 2009.

[19] Calì, M., Santarelli, M., and Leone, P., "Computer Experimental Analysis of the CHP Performance of a 100 kWe SOFC Field Unit by a Factorial Design," *Journal of Power Sources*, Vol. 156, pp. 400–413. doi:10.1016/j.jpowsour.2005.06.033, 2006.

[20] Calì, M., Santarelli, M., and Leone, P., "Design of Experiments for Fitting Regression Models on the Tubular SOFC CHP100 kWe: Screening Test, Response Surface Analysis and Optimization," *International Journal of Hydrogen Energy*, Vol. 32, pp. 343–358. doi:10.1016/j.ijhydene.2006.05.021, 2007.

[21] Leone, P., Lanzini, A., Squillari, P., Asinari, P., Santarelli, M., Borchiellini, R., and Calì, M., "Experimental Evaluation of the Operating Temperature Impact on Solid Oxide Anode-Supported Fuel Cells," *International Journal of Hydrogen Energy*, Vol. 33, pp. 3167–3172. doi:10.1016/j.ijhydene.2008.03.042, 2008.

[22] Leone P., et al., "Microstructural Characterization of SOFC Electrodes and Related Degradation Phenomena Through Image Analysis Techniques," Politecnico di Torino, Torino, Italy, 2009.

[23] Asinari, P., Calì, M., von Spakovsky, M., and Kasula, B., "Direct Numerical Calculation of the Kinematic Tortuosity of Reactive Mixture Flow in the Anode Layer of Solid Oxide Fuel Cells by the Lattice Boltzmann Method," *Journal of Power Sources*, Vol. 170, pp. 359–375. doi:10.1016/j.jpowsour.2007.03.074, 2007.

[24] Chen, X. J., Chan, S. H., and Khor, K. A., "Simulation of a Composite Cathode in Solid Oxide Fuel Cells," *Electrochimica Acta*, Vol. 49, pp. 1851–1861. doi:10.1016/j.electacta.2003.12.015, 2004.

[25] Santarelli, M., Cabrera, M., and Calì, M., "SOFC-Based Systems as APU for Regional Jets: A Feasibility Analysis," *ECS Transactions*, Vol. 17 No. 1, pp. 197, 2009.

[26] Shavit, Z., et al., "Parametric Sizing of a More-Electric Regional Jet Aircraft," Politecnico di Torino, ENFICA-FC Rept. D2/5, Torino, Italy, 2007.